

Title	Detection and engineering of spatial mode entanglement with ultracold bosons
Authors	Goold, John;Heaney, Libby;Busch, Thomas;Vedral, Vlatko
Publication date	2009
Original Citation	Goold, J., Heaney, L., Busch, T. and Vedral, V. (2009) 'Detection and engineering of spatial mode entanglement with ultracold bosons', Physical Review A, 80(2), 022338 (5pp). doi: 10.1103/PhysRevA.80.022338
Type of publication	Article (peer-reviewed)
Link to publisher's version	https://journals.aps.org/pr/abstract/10.1103/PhysRevA.80.022338 - 10.1103/PhysRevA.80.022338
Rights	© 2009, American Physical Society
Download date	2025-09-03 05:01:23
Item downloaded from	https://hdl.handle.net/10468/4534

Detection and engineering of spatial mode entanglement with ultracold bosons

J. Goold,^{1,*} Libby Heaney,^{2,†} Th. Busch,¹ and V. Vedral^{2,3}¹*Department of Physics, University College Cork, Cork, Republic of Ireland*²*Centre for Quantum Technologies, National University of Singapore, 3 Science Drive 2, Singapore 117543, Singapore*³*School of Physics and Astronomy, University of Leeds, Leeds LS2 9JT, United Kingdom*

(Received 12 February 2009; published 28 August 2009)

We outline an interferometric scheme for the detection of bimode and multimode spatial entanglement of finite-temperature interacting Bose gases. Whether entanglement is present in the gas depends on the existence of the single-particle reduced density matrix between different regions of space. We apply the scheme to the problem of a harmonically trapped repulsive boson pair and show that while entanglement is rapidly decreasing with temperature, a significant amount remains for all interaction strengths at zero temperature. Thus, by tuning the interaction parameter, the distribution of entanglement between many spatial modes can be modified.

DOI: [10.1103/PhysRevA.80.022338](https://doi.org/10.1103/PhysRevA.80.022338)

PACS number(s): 03.67.Bg, 03.75.Gg, 03.67.Mn, 67.10.Ba

I. INTRODUCTION

Understanding and controlling entanglement in many-body systems is one of the most important challenges in quantum mechanics today. The rewards are significant and are expected to not only lead to new insights into the properties of solid-state systems and phase transitions [1], but also to new designs for highly efficient quantum information devices. Ultracold bosonic gases offer an ideal arena to explore many-body entanglement, as experimentalists have at their disposal *designer* condensed-matter systems whose parameters can be controlled with unprecedented precision [2].

Entanglement often exists naturally in the ground state of a many-body system [3], where it resides between the degrees of freedom of the particles and is a property of the first quantized many-body wave function. However, in ultracold gases the particles are inherently indistinguishable, which requires the symmetrization of their many-body wave function and means that the Hilbert space no longer has the tensor product structure required to define entanglement. The first quantized many-body wave function of indistinguishable particles may therefore contain quantum correlations [4], but such correlations are usually considered unable to violate a Bell inequality or to process quantum information [4–6].

Ultracold gases are also well described within the framework of second quantization where, instead of working directly with the many-body wave function, one defines a complete set of field modes that are occupied by particles. Second quantization therefore offers the possibility of entanglement between modes. Entanglement is dependent on the choice of modes and provided the correct choice is made, investigating entanglement between *distinguishable* modes [7–9] circumvents the difficulties of defining entanglement between indistinguishable particles [10,11].

To illustrate the differences between particle and mode entanglement, let us consider two noninteracting bosons in a trap at zero temperature. In first quantization, the wave function is the symmetrized product $\Psi_{12}(x,y) = \frac{1}{\sqrt{2}}[\phi_1(x)\phi_2(y)$

$+\phi_1(y)\phi_2(x)]$, where $\phi(x)$ is the ground state of the confining potential. No entanglement exists between the particles, since indistinguishability forbids us from assigning to any particle a specific set of degrees of freedom. Conversely, in second quantization one can define a pair of spatial modes, A and B , where each mode occupies half the confining geometry. Since both the particles are coherently distributed over these modes, the system is described by the entangled state $|\psi_{AB}\rangle = \frac{1}{2}(|20\rangle + \sqrt{2}|11\rangle + |02\rangle)$, where $|mn\rangle = |m\rangle_A \otimes |n\rangle_B$ denotes m particles in mode A and n particles in mode B (with $m+n=2$).

In this paper we outline a scheme for the detection of bimode and multimode spatial entanglement for a finite-temperature interacting Bose gas of any (including unknown) particle number. We show that entanglement is detected via the single-particle reduced density matrix (SPRDM). We apply our scheme to the example of a harmonically trapped interacting boson pair [12], where the SPRDM also acts as a quantifier of entanglement. We find that, for all interaction strengths, entanglement between pairs of modes rapidly decreases with temperature, while at zero temperature a significant amount of entanglement remains even in the limit of infinite interaction. Moreover, we note that our detection scheme is also relevant to recent proposals to observe non-locality of single particle between spatial modes [13,15].

II. DETECTION SCHEME

The correlations of entanglement are locally basis independent, so that one needs to measure each mode in at least two bases in order to differentiate them from classical correlations. While a superselection rule that forbids coherent superpositions of eigenstates of different mass [14] seems to rule such measurements out for any atomic system, recent work has shown that such measurements are theoretically possible [15]. Moreover, it has recently been predicted that this natural mode entanglement of massive particles can be used as a resource for quantum communication [16]. However, in practice it will be difficult to locally manipulate, i.e., to rotate, the spatial modes. In the following we will show that spatial entanglement can also be detected and quantified by making *global* operations on the modes.

*jgoold@phys.ucc.ie

†l.heaney1@physics.ox.ac.uk

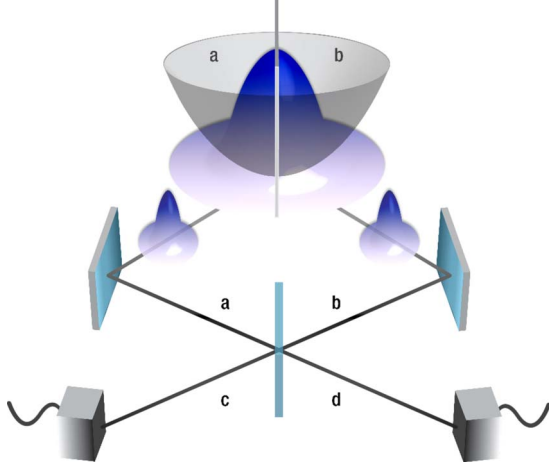


FIG. 1. (Color online) Schematic showing a trapped wave function split into two spatial modes a and b . The modes are combined at a 50:50 beam splitter and the particles in the output modes c and d are counted.

Let us consider a gas in a confining geometry (see Fig. 1) which is mathematically, but not necessarily physically, divided into two nonoverlapping spatial modes a and b . The field operators $\hat{\psi}_i^\dagger = \int d\vec{x} g^*(\vec{x}) \hat{\psi}^\dagger(\vec{x})$ and $\hat{\psi}_i = \int d\vec{x} g(\vec{x}) \hat{\psi}(\vec{x})$ create and destroy particles in mode $i=a, b$, where $\int |g(\vec{x})|^2 d\vec{x} = 1$ ensures that the commutation relations $[\hat{\psi}_i, \hat{\psi}_j^\dagger] = \delta_{ij}$ are satisfied. The quantity $g(\vec{x})$ specifies how the set of points in a spatial mode are averaged over. To generate interference, the particles in the two spatial modes a and b are mixed at a 50:50 beam splitter, which transforms the input modes as $\hat{\psi}_a^\dagger = \frac{1}{\sqrt{2}}(\hat{\psi}_c^\dagger + \hat{\psi}_d^\dagger)$ and $\hat{\psi}_b^\dagger = \frac{1}{\sqrt{2}}(\hat{\psi}_c^\dagger - \hat{\psi}_d^\dagger)$. After the beam splitting operation, the number of particles in the output modes c and d are counted and compared to the fully separable case. If the number of coincidences is different to the separable case, we can conclude that there must have been entanglement between the spatial modes.

A bosonic gas of fixed particle number N , which is in a fully separable state with respect to the spatial modes a and b , can be written as

$$\hat{\rho}_{sep} = \sum_{n=0}^N p_n |n\rangle \langle n|_a \otimes |N-n\rangle \langle N-n|_b, \quad (1)$$

where $\sum_n p_n = 1$. The beam splitter transforms this state such that if the total number of particles is even, one detects the same number of particles in each of the output modes, i.e., $\Delta N = |N_c - N_d| = 0$. For an odd number of particles an ensemble average leads to the same result [17].

Conversely, if the initial state of fixed particle number is of an arbitrary form $\hat{\rho}$, the difference in particle numbers detected in modes c and d may be nonzero due to entanglement between the modes,

$$\Delta N = |\text{tr}[\hat{\psi}_c^\dagger \hat{\psi}_c \hat{\rho}] - \text{tr}[\hat{\psi}_d^\dagger \hat{\psi}_d \hat{\rho}]| = 2|\epsilon_{ab}|, \quad (2)$$

where

$$\epsilon_{ab} = \text{tr}[\hat{\psi}_a^\dagger \hat{\psi}_b \hat{\rho}] = \int_a d\vec{x} \int_b d\vec{x}' g(\vec{x}) g^*(\vec{x}') \rho^{(1)}(\vec{x}, \vec{x}'). \quad (3)$$

We have derived the above result using the Fourier decomposition of the field operators $\hat{\psi}^\dagger(\vec{x})$ and $\hat{\psi}(\vec{x})$ in terms of the momentum modes $\phi_k(\vec{x})$, as $\hat{\psi}^\dagger(\vec{x}) = \sum_k \phi_k^*(\vec{x}) \hat{a}_k^\dagger$ and likewise for $\hat{\psi}(\vec{x})$. When ϵ_{ab} is nonzero, the state $\hat{\rho}$ is different to the separable case and is therefore necessarily entangled with respect to the bimodal split into a and b .

The quantity ϵ_{ab} is given by the off-diagonal elements of the SPRDM, which is defined as $\rho^{(1)}(\vec{x}, \vec{x}') = \sum_{\vec{k}} n_{\vec{k}} \phi_{\vec{k}}(\vec{x}) \phi_{\vec{k}}^*(\vec{x}')$. Here, $n_{\vec{k}}$ is the number of bosons that occupy the k th momentum mode. The SPRDM is a one-body correlation function, which characterizes important coherence properties of a many-body system [18] and its off-diagonal elements are related to the visibility of interference fringes in a two-slit experiment [19].

Our scheme therefore applies to systems whose correlations form a basic group of one particle [20]. States of the form $|20\rangle + |02\rangle$, whose correlations are second order, are not detected by the SPRDM. Such states require careful engineering of bosonic systems [21], although they may form naturally in fermionic systems, i.e., Cooper pairs in superconductors. Our scheme is applicable to all bosonic gases trapped in orthodox geometries.

Next, let us show that ϵ_{ab} can also be used to *quantify* mode entanglement for certain systems, one of which is the boson pair model discussed below. For this, ϵ_{ab} must fulfill three basic criteria [22]: (i) ϵ_{ab} is zero when the state is separable, (ii) ϵ_{ab} is invariant under local unitary operations, and (iii) ϵ_{ab} does not increase under local general measurements and classical communication (LGM+CC). The validity of (i) is shown above and (ii) is guaranteed since the trace is basis independent. One can prove (iii) as follows. To implement LGM+CC, the two spatial modes a and b are each coupled to a local environment by a general completely positive map. The environments are allowed to communicate classically *ad infinitum* and the total number of particles in the gas and environment is fixed. One can then show that ϵ_{ab} does not increase under LGM+CC.

The above scheme can also analyze multimode entanglement, i.e., the simultaneous entanglement of more than two modes. In the following we use the different notions of separability discussed in [23]. A general M -mode state is fully separable and contains no entanglement if it is a convex combination of states for each mode, $\hat{\rho}_{sep(M)} = \sum_i p_i \hat{\rho}_i^{(1)} \otimes \cdots \otimes \hat{\rho}_i^{(M)}$. Here, each composite state $\hat{\rho}_i^{(j)}$ corresponds to a single spatial mode with a fixed number of particles. On the other hand, entanglement may be present between certain subsets of spatial modes, for which one can define a p -separable state $\hat{\rho}_{sep(p)} = \sum_i p_i \hat{\rho}_i^{(1)} \otimes \cdots \otimes \hat{\rho}_i^{(p)}$, where $p \leq M$ with equality when the state is fully separable as above. When the composite state $\hat{\rho}_i^{(j)}$ describes more than one spatial mode, the spatial modes contained within $\hat{\rho}_i^{(j)}$ are necessarily entangled; otherwise, $\hat{\rho}_i^{(j)}$ would be written as a product of states for the individual modes, $\hat{\rho}_i^{(j)} = \hat{\rho}_i^{(j_1)} \otimes \cdots \otimes \hat{\rho}_i^{(j_d)} \otimes \cdots$, and the overall state of the system would be σ separable, where $p < \sigma \leq M$ [23].

To determine whether a given M -mode state contains multimode entanglement, one can check a bipartite entanglement criterion between all $2^{M-1}-1$ unique divisions of the system into two *blocks* A and B . Depending on which pairs of blocks are found to be separable, one can conclude that the state has entanglement between different subsets of spatial modes. Here, the bipartite entanglement criterion is $\epsilon_{AB} = \text{tr}[\hat{\Psi}_A^\dagger \hat{\Psi}_B \hat{\rho}]$ of Eq. (3), i.e., the SPRDM between two blocks of spatial modes, A and B . The field operators $\hat{\Psi}_X^\dagger$ and $\hat{\Psi}_X$ for blocks of spatial modes are defined as $\hat{\Psi}_X^\dagger = \sum_{i \in X} c_i^\dagger \hat{\psi}_i^\dagger$ and $\hat{\Psi}_X = \sum_{i \in X} c_i \hat{\psi}_i$, where $X=A, B$ and $\sum_{i \in A} |c_i|^2 = 1$ ensures that the commutation relations $[\hat{\Psi}_X, \hat{\Psi}_Y^\dagger] = \delta_{X,Y}$ are satisfied.

We now describe how entanglement changes for (i) the fully separable, (ii) the p -separable, and (iii) the fully entangled states: (i) The fully separable state $\hat{\rho}_{\text{sep}(M)}$ admits no interference between all $2^{M-1}-1$ partitions into blocks, i.e., $\epsilon_{AB}=0$ for all A and B . (ii) A p -separable state $\hat{\rho}_{\text{sep}(p)}$, where $p < M$, admits no interference for $2^{p-1}-1$ partitions into blocks from the total of $2^{M-1}-1$ partitions, i.e., $\epsilon_{AB}=0$ for $2^{p-1}-1$ choices of A and B . (iii) A fully entangled state $\hat{\rho} = \sum_i p_i \hat{\rho}_i$ admits interference for all $2^{M-1}-1$ choices of blocks, i.e., $\epsilon_{AB} \neq 0$ for all A and B . The fully entangled state $\hat{\rho}$ necessarily contains some forms of multimode entanglement, since otherwise there would exist a decomposition such that $\hat{\rho}$ is p separable.

III. BOSON PAIR MODEL

In the following we will apply our scheme to the physically realistic model of a harmonically trapped pair of ultra-cold interacting bosonic atoms in effectively one dimension. The Hamiltonian of such a system is given by

$$\hat{H} = \sum_{i=1}^2 \left(-\frac{1}{2} \frac{d^2}{dx_i^2} + \frac{1}{2} x_i^2 \right) + g_{1D} \delta(|x_i - x_j|), \quad (4)$$

where all lengths are scaled in units of the ground-state size and all energies are scaled in units of the harmonic frequency. The one-dimensional coupling constant g_{1D} is related to the three-dimensional s -wave scattering length by $g_{1D} = (\hbar^2 a_{3D} / m a_\perp) (a_\perp - C a_{3D})^{-1}$, where C is the constant, $C = 1.4603$ [24]. This Hamiltonian can be decoupled by moving into the center of mass and relative coordinate frames labeled by X and x , respectively [12], and the two-body wave function can subsequently be written as $\Psi_{n,\nu}(x_1, x_2) = \psi_n(X) \psi_\nu(x)$. The eigenvalues for the center of mass motion are given by $\epsilon_n^{\text{com}} = (n + \frac{1}{2})$ for $n=0, 1, \dots$, with corresponding eigenstates $\psi_n^{\text{com}}(X) = \mathcal{N}_n H_n(X) e^{-X^2/2}$. Here, \mathcal{N}_n is the normalization constant and $H_n(X)$ are the Hermite polynomials. For the relative motion, the single-particle eigenstates are $\psi_\nu^{\text{rel}}(x) = \mathcal{N}_\nu e^{-x^2/2} U(\frac{1}{4} - E_\nu/2, \frac{1}{2}, x^2)$, where $\nu=0, 2, 4, \dots$ and $U(a, b, z)$ are the confluent hypergeometric functions. The corresponding eigenenergies E_ν are determined by the roots of the implicit relation $-g_{1D} = 2[\Gamma(-E_\nu/2 + \frac{3}{4}) / \Gamma(-E_\nu/2 + \frac{1}{4})]$ [12]. The kernel of the density operator in position representation is $\rho_{n\nu}(x, x', x_2) = \Psi_{n,\nu}^*(x, x_2) \Psi_{n,\nu}(x', x_2)$, with the SPRDM defined as $\rho_{n\nu}^{(1)}(x, x') = \int_{-\infty}^{+\infty} \rho_{n\nu}(x, x', x_2) dx_2$. The

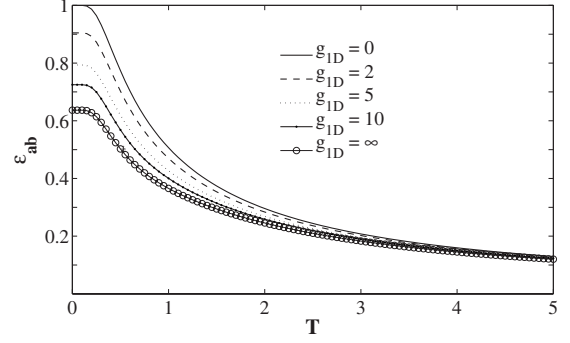


FIG. 2. Amount of entanglement between two spatial regions occupied by a boson pair as specified in the text as a function of temperature. The values of the dimensionless interaction parameter increase from the top curve to the bottom curve as $g_{1D} = 0, 2, 5, 10, \infty$. Temperature is scaled in units of $\hbar \omega / k_B$.

SPRDM in thermal equilibrium is given by $\rho^{(1)}(x, x') = \sum_n \sum_\nu P_{n\nu} \rho_{n\nu}^{(1)}(x, x')$, where $P_{n\nu}$ is the Boltzmann weight, $P_{n\nu} = \frac{1}{Z} \exp(-E_{n\nu} / k_B T)$, k_B is the Boltzmann constant, and Z is the partition function.

IV. BIMODE AND MULTIMODE ENTANGLEMENT RESULTS

We define two equal length modes a and b and calculate their spatial entanglement for the boson pair model as a function of temperature and interaction strength using Eq. (3). The results are displayed in Fig. 2. With increasing temperature, the gas becomes a statistical mixture of momentum modes, $\phi_k(x)$, which destroys the fixed relative phase between the spatial modes and consequently the entanglement between them is severely depleted. The presence of interaction also degrades the quality of the entanglement at $T=0$, but a significant amount persists even in the Tonks-Girardeau limit, of impenetrable bosons, $g_{1D}=\infty$. At first this may seem surprising, since in the Tonks-Girardeau limit the system can be mapped onto an ideal fermionic atom pair [25], for which one may not expect any entanglement to be present. However, only the local properties of the bosons become identical to free spin-polarized fermions due to the Bose-Fermi mapping and therefore entanglement is not affected.

We also examine pairwise entanglement in this model. For this, the space is divided into three modes, a , b , and c , and we check entanglement between all pairs, ab , bc , and ac , as a function of the interaction strength at zero temperature. The results are shown in Fig. 3, where three different central mode lengths L_b are considered. The left graph of Fig. 3 shows entanglement between neighboring modes, ab (and for symmetry reasons bc). Here, the entanglement decreases as the interaction strength g_{1D} increases for all lengths studied. The right-hand side graph of Fig. 3 shows the entanglement between outer modes a and c . The entanglement increases initially for all mode sizes as the interaction strength is varied. For the central mode size of $L_b=1.4$, entanglement however is not a monotonic function of g_{1D} and decreases after the initial rise. For $L_b=2.8$ and 4, this is not the case. The behavior of entanglement in both graphs can be ex-

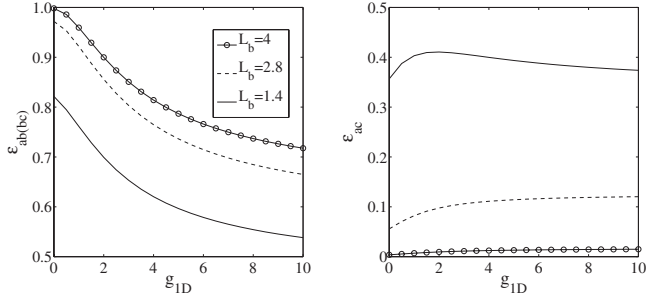


FIG. 3. The system is split into three spatial modes a , b , and c . Mode a is defined as the region $-\infty < x < -L_b/2$, mode b as $-L_b/2 < x < L_b/2$, and mode c as $L_b/2 < x < \infty$. Entanglement is investigated between neighboring modes a and b (b and c) (left-hand side) and also between the outer two modes a and c (right-hand side) at $T=0$ as the interaction is varied. Three different central mode lengths $L_b=4, 2.8, 1.4$ are taken.

plained by the delocalization of the bosons away from the center of the trap due to greater interaction strengths. Stronger interaction therefore increases the correlation length (i.e., the entanglement between the outer two modes), yet decreases the overall coherence of the sample.

We also check the existence of multimode entanglement in our model. For this we have divided our two-particle wave function into M modes and calculated ϵ_{AB} for the $2^{M-1}-1$ unique partitions of these modes into two blocks A and B . Recall that ϵ_{AB} must be nonzero for all possible block combinations for the state to be fully entangled. We have found that at zero temperature the system possesses full multimode entanglement, i.e., $\epsilon_{AB} \neq 0$ for all A and B , for a wide range of values of the interaction parameter, provided that the set of modes are defined within the coherence length of the sample.

Here, we have used the repulsively interacting boson pair model to illustrate our scheme, since it is analytically tractable and contains all the essential features of larger models. Our scheme to detect bimode and multimode entanglement can also be applied to Bose gases with a greater number of particles (for all interaction strengths and temperatures), but qualitatively the results will remain unchanged while the task of computing the single-particle reduced density matrix between modes will quickly become very demanding. We note that bimode entanglement of a noninteracting Bose gas has been studied before for N particles at zero [7] and at finite [26] temperatures.

Our scheme can be implemented using currently available technologies. Atomic beam splitters can be realized with optical potentials [27] and separate modes can be defined using spatially selective out-coupling techniques [19]. To perform beam splitting on systems with strong interactions, one should raise a potential barrier between the desired modes on a nonadiabatic time scale, so that the coherences between the regions are not lost (i.e., so that the gas does not enter a Mott-like state). The potential barrier should then be lowered rapidly enough, so that the coupling between the wells is greater than the on-site interaction energy of the wells. For instance, one could envisage a setup where the trap is swiftly modulated from harmonic to double-well potential and is then switched off and the sample left to interfere. The entanglement can be inferred according to Eq. (3) from the visibility of the resulting interference fringes (see, for example, [19,28]), where mode entanglement between regions of space has already been measured indirectly.

V. CONCLUSIONS

We have outlined a scheme that detects bimodal and multimodal spatial entanglement of cold bosonic gases using simple atom-optic techniques. We show that spatial entanglement is detected by the SPRDM between different modes, a quantity that is related to the visibility of routinely measured interference fringes. We have demonstrated our scheme using the model of a harmonically trapped boson pair and have found the existence of bimode and multimode entanglement within the gas. For all interaction strengths, increasing temperature rapidly degrades the amount of entanglement, but at zero temperature entanglement still remains, even in the presence of strong interactions. Therefore, we have shown that the ability to vary the particle interaction strength allows one to engineer the distribution of entanglement over the trap, thus allowing a tunable source of entanglement.

ACKNOWLEDGMENTS

The authors would like to thank J. Anders, P. Turner, W. Son, and M. Paternostro for valuable discussions. J.G. and T.B. acknowledge funding from Science Foundation Ireland Project No. 05/IN/I852. L.H. and V.V. are funded by the National Research Foundation (Singapore) and the Ministry of Education (Singapore).

- [1] L. Amico, R. Fazio, A. Osterloh, and V. Vedral, *Rev. Mod. Phys.* **80**, 517 (2008).
- [2] I. Bloch, J. Dalibard, and W. Zwerger, *Rev. Mod. Phys.* **80**, 885 (2008).
- [3] K. Audenaert, J. Eisert, M. B. Plenio, and R. F. Werner, *Phys. Rev. A* **66**, 042327 (2002).
- [4] R. Păskauskas and L. You, *Phys. Rev. A* **64**, 042310 (2001).
- [5] H. M. Wiseman and J. A. Vaccaro, *Phys. Rev. Lett.* **91**, 097902 (2003).

- [6] M. R. Dowling, A. C. Doherty, and H. M. Wiseman, *Phys. Rev. A* **73**, 052323 (2006).
- [7] C. Simon, *Phys. Rev. A* **66**, 052323 (2002).
- [8] L. Heaney, Ph.D. thesis, University of Leeds, 2008.
- [9] J. Estève, C. Gross, A. Weller, S. Giovanazzi, and M. K. Oberthaler, *Nature (London)* **455**, 1216 (2008).
- [10] B. Sun, D. L. Zhou, and L. You, *Phys. Rev. A* **73**, 012336 (2006).
- [11] D. S. Murphy, J. F. McCann, J. Goold, and Th. Busch, *Phys.*

- Rev. A **76**, 053616 (2007).
- [12] Th. Busch, B.-G. Englert, K. Rzażewski, and M. Wilkens, *Found. Phys.* **28**, 549 (1998).
 - [13] J. Dunningham and V. Vedral, *Phys. Rev. Lett.* **99**, 180404 (2007).
 - [14] S. D. Bartlett, T. Rudolph, and R. W. Spekkens, *Rev. Mod. Phys.* **79**, 555 (2007).
 - [15] L. Heaney and J. Anders, e-print arXiv:0810.2882, *Phys. Rev. A* (to be published).
 - [16] L. Heaney and V. Vedral, e-print arXiv:0907.5404.
 - [17] It is worth noting that this criterion means that the exact number of particles (which tends to be unknown in cold atom experiments and varies between different experimental runs) does not matter.
 - [18] O. Penrose and L. Onsager, *Phys. Rev.* **104**, 576 (1956).
 - [19] I. Bloch, T. W. Hänsch, and T. Esslinger, *Nature (London)* **403**, 166 (2000).
 - [20] Note that a basic group was defined by Yang [C. N. Yang, *Rev. Mod. Phys.* **34**, 694 (1962)] as the smallest collection of particles that give rise to the correlations in a system.
 - [21] S. Fölling, S. Trotzky, P. Cheinet, M. Feld, R. Saers, A. Widera, T. Müller, and I. Bloch, *Nature (London)* **448**, 1029 (2007).
 - [22] V. Vedral, M. B. Plenio, M. A. Rippin, and P. L. Knight, *Phys. Rev. Lett.* **78**, 2275 (1997).
 - [23] E. Shchukin and W. Vogel, *Phys. Rev. A* **74**, 030302(R) (2006).
 - [24] M. Olshanii, *Phys. Rev. Lett.* **81**, 938 (1998).
 - [25] M. Girardeau, *J. Math. Phys.* **1**, 516 (1960).
 - [26] L. Heaney, J. Anders, D. Kaszlikowski, and V. Vedral, *Phys. Rev. A* **76**, 053605 (2007).
 - [27] K. Bongs and K. Sengstock, *Rep. Prog. Phys.* **67**, 907 (2004).
 - [28] S. Hofferberth, I. Lesanovsky, B. Fischer, T. Schumm, and J. Schmiedmayer, *Nature (London)* **449**, 324 (2007).